The atmospheric boundary layer structure over the open and ice-covered Baltic Sea: In situ measurements compared to simulations with the regional model REMO

Burghard Brümmer[1], Amélie Kirchgäßner[2] and Gerd Müller[1]

[1]Meteorological Institute, University of Hamburg, Germany
[2]British Antarctic Survey, Cambridge, UK

3 March 2008

Abstract

The regional model REMO which is the atmospheric component of the coupled atmosphere-ice-ocean-land climate model system BALTIMOS is tested with respect to its ability to simulate the atmospheric boundary layer over the open and ice-covered Baltic Sea. REMO simulations are compared to ship, radiosonde and aircraft observations taken during eight field experiments. The main results of the comparisons are: (1) Sharpness and strength of the temperature inversion are underestimated by REMO. Over open water, this is connected with an overestimation of cloud coverage and moisture content above the inversion. (2) The vertical temperature stratification in the lowest 200 m over sea ice is too stable. (3) The horizontal inhomogeneity of sea ice concentration as observed by aircraft could not properly be represented by the prescribed ice concentration in REMO; large differences in the surface heat fluxes arise especially under cold-air advection conditions. The results of the comparisons suggest a reconsideration of the parameterisation of subgrid-scale vertical exchange both under unstable und stable conditions.

1. Introduction

Regional coupled models of the atmosphere, ocean, sea ice and land system are increasingly used as a method to estimate the climate on the regional scale. Since observations can never be complete in space and time, coupled models are a promising tool. However, the accuracy of the models has to be known and determined by comparisons with independent observations which did not enter into the model as initial or boundary conditions. Basically, model validation is a comprehensive task and can never be complete but only cover restricted aspects.

In this paper, the regional model REMO which is the atmospheric component of the coupled (atmosphere, ocean, sea ice, land) model system BALTIMOS (BALTEX Integrated Model System; Jacob et al., 2006; Lorenz and Jacob, 2006) is tested with respect to its ability to simulate the atmospheric boundary layer (ABL) over the open and ice-covered Baltic Sea. The Baltic Sea and its catchment area is one focus of regional climate research, which is coordinated within the BALTEX (Baltic Sea Experiment) project (BALTEX, 1995) which in turn is embedded within the WCRP (World Climate Research Programme) GEWEX (Global Energy and Water Cycle Experiment, e.g. WCRP, 1991; Sorooshian et al., 2005). Compared to the catchment area, the Baltic Sea itself is an area with rather few observations. To overcome this deficiency and to gain an independent observational data set for comparison with REMO, eight field experiments over the Baltic Sea were conducted. The comparisons concentrate on the vertical structure of the ABL. Primarily the temperature inversion is a decisive quantity which determines the vertical transport of momentum, heat and moisture, the generation of clouds and thus the radiation and energy budget at the surface. A study with a similar objective as in this paper was made by Pirazzini et al. (2002). Using measurements from two field campaigns over the open and ice-covered Baltic Sea in 1999 they validated the boundary layer structure as simulated by the operational atmospheric model HIRLAM of the Finnish Meteorological Institute.

This paper is organized as follows. The special observations which were made are described in Section 2 and the corresponding REMO simulations are presented in Section 3. Comparisons between REMO and observations for the open and the ice-covered Baltic Sea are displayed in Sections 4 and 5, respectively. A resume and conclusions are given in Section 6.

2. ABL observations over the Baltic Sea

The ABL observations used in this paper were taken during eight so-called BALTIMOS field experiments. The experiments were systematically distributed over the year; each season was covered by two experiments. Six experiments took place over the open water in the middle of the Baltic Sea proper in April, June and October in 2000 and 2001. Two experiments were conducted over the ice-covered northern part of the Baltic Sea, the Bay of Bothnia, in February/March 1998 and February 2001. The locations of the field experiments are shown in Fig. 1. The eight BALTIMOS field experiments are described in detail in Brümmer et al. (2003).

The following platforms and instrumentation were involved. The six field experiments over the Baltic Sea proper were performed with the German research vessel (RV) Alkor. Continuous measurements on board the ship and 3 to 6-hourly Vaisala radiosonde measurements were taken. During the two winter campaigns, the Finnish RV Aranda was placed within the land-fast sea ice at several kilometres distance from the land, and in addition a coastal station (CS) was installed on the sea ice in about 100 m distance from the shore and a research aircraft (RA) was involved. From RV Aranda continuous surface layer measurements as well as 3-hourly radiosonde measurements were taken. During the 1998 winter campaign a CS was installed near Kokkola from where continuous

observations in the surface layer and 3-hourly radiosonde observations were performed. During the 2001 winter campaign a CS was installed near Marjaniemi on the island of Hailuoto. There, continuous surface layer observations were taken. Aircraft measurements of the 3-dimensional state of the ABL over sea ice around the areas of RV Aranda and the respective CS were performed in winter 1998 by the German RA Falcon and in winter 2001 by the German RA DO-128. The locations of RV Aranda, the CS and the areas of the aircraft operations are shown in Fig. 1.

The meteorological quantities used in this paper for comparison with REMO are listed in Table 1 together with the corresponding accuracy. The accuracies refer to specifications of the instrument manufactures and the platform (ship, aircraft) operating companies. The accuracy of a certain quantity measured at different platforms is rather similar because the same instrument type or measurement principle was used.

3.   Simulations with the regional model REMO

The regional model REMO is described in detail e.g. in Jacob et al. (2001) and Jacob (2001). For the purpose of model validation in this study, REMO was run for an area of about 3000 km (north-south) by 2000 km (east-west) enclosing the Baltic Sea and its catchment area. The horizontal grid resolution is $\Delta x = 1/6°$. In vertical direction, 21 levels are applied; 5 levels are placed below 1000 m ($z \approx 30, 130, 310, 520, 740$ m). The time step is $\Delta t = 100$ seconds. The boundary conditions are taken from the analyses of the actual ECMWF (European Centre for Medium-range Weather Forecast) model and are renewed every 6 hours. The initial conditions are also taken from the ECMWF analyses.

REMO can be run in two modes: either the climate or the forecast mode. In the climate mode, initial conditions are prescribed only once and the model integrates over long periods (months, years or even longer). In the forecast mode, initial conditions are prescribed at regular time intervals and the model starts a new integration every time. For the ABL validation in this study, REMO was run in the forecast mode. Initial conditions were prescribed daily at 00 UTC and each individual forecast covered a period of 30 hours. Since after the start of a new integration the model needs some time to adjust to the new initial conditions, the first 6 hours of each integration were neglected.

In this way, a continuous time series was constructed by combining the 24 hours long short-range forecasts (from hour 7 to hour 30 of the forecast period). This was done for the duration of each of the eight BALTIMOS field experiments. The results of the REMO runs in the forecast mode were stored every full hour. In the case that the in situ observations were not taken at the full hour or at a model grid point, REMO data were interpolated for the respective time and location of measurements.

REMO uses a boundary layer scheme with a local closure of order 1.5. Eddy diffusivity and transfer coefficient are stability dependent and different for momentum and heat flux. The lower boundary conditions were taken from ECMWF analyses. This concerns the surface temperature of open water, T_w. The area fraction of the sea ice, n_{ice}, was taken from the sea ice maps of the Finnish Institute of Marine Research (FIMR), Helsinki. For this purpose the ice maps had to be digitized for the REMO grid. T_w and n_{ice} are kept constant during each REMO integration. The surface temperature of sea ice, T_{ice}, is calculated within REMO by means of a simple energy balance model. For this purpose the ice was assumed to be 0.5 m thick without a snow layer on top. The thermal conductivity of sea ice was assumed as 2.0 $Wm^{-1} K^{-1}$ and the albedo of sea ice as 0.75 for $T_{ice} < -10°$ C, as 0.50 for $T_{ice} > 0°$ C with a linear variation between -10 and 0° C.

4. Comparison over open water

Comparisons were performed separately for the measurements taken in the surface layer (SL) on board the RV Alkor and for the radiosoundings. SL measurements were recorded continuously (1 minute averages). For comparison with REMO, 10-min averages were used centred at every full hour. For comparison with radiosondes, REMO data were time interpolated. However, the varying time with height during the radiosonde ascent was not taken into account, because only the ABL (the radiosonde passes through the lowest 1.5 km in about 5 minutes) is considered here. Concerning position, REMO data were interpolated to the measurement position according to the distance weighted average of the four surrounding model grid points.

4.1. Surface layer comparison

Table 2 summarizes the results of the SL comparisons for various quantities. The mean differences (REMO minus observation) are remarkably small for air temperature $\left(|\Delta T| < 0.8\,\text{K}\right)$, relative humidity $\left(|\Delta RH| < 9\,\%\right)$, surface temperature $\left(|\Delta T_s| < 1.1\,\text{K}\right)$ and wind speed $\left(|\Delta FF| < 1.6\,\text{ms}^{-1}\right)$ during each field experiment. Air pressure and wind direction differences are partly large for some experiments, but have no uniform bias. However, a clear bias is obvious for downwelling shortwave and longwave radiation and cloud cover (measured by a ceilometer). The differences for the latter three quantities have consistently the same sign during all experiments. This hints at an overestimation of clouds in REMO resulting in consequences on the radiation fluxes: more clouds reduce shortwave radiation and raise longwave radiation.

4.2. Comparison of vertical ABL structure

The temperature inversion is an important feature of the ABL structure. It limits the vertical turbulent and convective exchange of heat, moisture and momentum. The comparison of the temperature inversion between model and observation, thus, delivers important indications about the ability of the model to represent vertical exchange processes (turbulence, convection, cloud formation).

In Table 3 the results of the temperature inversion comparison are presented. They are based on 154 radiosondes during the six field experiments. Altogether, the frequency of inversions in the ABL is slightly less in REMO (100) than observed (117). This underestimation holds for surface inversions as well as elevated inversions. Concerning the inversion characteristics (base h_B, depth Δh, temperature increase ΔT), inversions are on average higher, deeper and weaker in REMO than observed.

In addition to the statistical comparison of the inversion characteristics in Table 3 we compare directly observed and modelled mean vertical profiles in Fig. 2. The profiles are classified into four categories with respect to the observed inversion base: (I) $h_B = 0$, (II) $h_B < 250$ m, (III) $h_B > 250$ m and (IV) no inversion below 1500 m. Each category is covered by approximately equal numbers of profiles to allow for a meaningful comparison between them. The different number of temperature/humidity profiles and wind profiles within each category is due to the fact that some radiosondes failed or had gaps in the wind measurement. Only wind profiles with vertically continuous data coverage are regarded in Fig. 2. The wind gap below 150 m was a general problem

of the GPS wind finding with the Vaisala radiosonde type used at that time, a problem which does not exist anymore with today's Vaisala radiosondes.

The observed mean profiles within each category were obtained by averaging with respect to the absolute height and not with respect to the height relative to the inversion. Thus, the primary inversion characteristics, temperature increase and vertical thickness, are represented in a "smoothed" way in Fig. 2 (this holds for the modelled inversion as well). The observed relative humidity profile is closely linked to the inversion and decreases in and above it. The observed wind in the ABL increases and veers with height. The vertical shear of both the wind speed and wind direction is the stronger the lower the inversion is located.

Temperature and relative humidity compare well in the SL in accordance to Table 2, but disagree systematically in the sub-inversion and inversion layer above. The stability in the inversion layer is underestimated in REMO and the stability in the sub-inversion layer is overestimated (categories I-III). Thus, in REMO a layer with strong stability which can hinder or at least reduce turbulent vertical exchange is missing. As a consequence moisture can be transported upward at a higher degree in REMO than observed and, thus, the largest positive moisture deviations occur in and above the inversion layer. Absolute values of the temperature and humidity differences between REMO and observations are not very large, but are distributed systematically with height.

In Fig. 2, the mean profiles of wind speed show differences between REMO and observations in all four categories, but the differences do not appear to be systematic. However, the differences in wind direction are striking and systematic. Wind direction has been "normalized" i.e. rotated so that the observed wind direction in the SL is zero. Thus, in Fig. 2 not the absolute wind direction but the relative wind direction (wind direction shear) is compared. The wind direction shear is systematically smaller in REMO than in the observations. This is confined to the inversion layer and sub-inversion layer. Above these layers, observed and modelled wind direction profiles run parallel and, thus, have the same shear. The underestimation of the vertical wind shear in REMO increases with decreasing observed inversion height and appears to be a further consequence of the underestimation of the stability in the ABL inversion. This results in a stronger (than in nature) vertical mixing of momentum and, thus, weaker vertical shear of wind direction.

5. Comparison over sea ice

Comparisons between REMO and observations over sea ice were performed in three ways: long-term observations at fixed places (RV Aranda, coastal station) over land-fast sea ice (1) in the SL and (2) in the ABL using radiosondes and (3) short-term snapshots of horizontal distributions in the SL and ABL from aircraft flights over heterogeneous sea ice.

The southern edge of the sea ice was located roughly in the same region during both winter experiments (see Fig. 1). In 1998 RV Aranda was placed rather close to the ice edge at a position with about 5 km distance from the coast, while in 2001 the vessel's position was much further into the ice and approximately 20 km off the coast. Both coastal stations, Kokkola and Marjaniemi, were located on the sea ice, but only about 100 m off the coast which in this region is flat and covered with coniferous forest.

5.1. Surface layer comparison

The results of the SL comparisons over sea ice are summarized in Table 4. They are based on 1335 hourly data pairs in total. At distant places from the ice edge (Aranda 2001, Kokkola and Marjaniemi) the SL air is colder, moister and flows at larger angles of deviation from the geostrophic flow (smaller values of wind direction) in REMO than observed. These three facts lead to the conclusion that the SL stability over sea ice is overestimated in REMO. This is supported by radiosonde profiles presented in Fig. 3. The overestimated SL stability in REMO cannot be attributed to the ice/snow surface temperature since it has no bias. An overestimation of cloud cover in REMO, as was the case over the open water (Table 2), can also be inferred to some extent from the comparisons of downwelling shortwave radiation over sea ice. The tendency of REMO to underestimate the downwelling shortwave radiation can also be found in the paper by Wyser et al. (2007), where REMO (together with seven other regional climate models) is compared to the one year long SHEBA (Surface Heat Budget of the Arctic Ocean) observations over the Arctic sea ice.

5.2. Comparison of vertical ABL structure

The comparison is based on 144 radiosondes launched either aboard RV Aranda in 1998 and 2001 or at the coastal station Kokkola in 1998. An ABL inversion below 1500 m was present in 132 profiles (91 %). In 84 profiles (58 %) the inversion was surface-based and in 48 cases (33 %) it was elevated. The ABL inversion over Baltic Sea ice is studied in detail in Brümmer et al. (2005). Another study on the Baltic Sea inversion is presented by Uotila et al. (1997). Again, as for the comparisons over open water, the radiosonde profiles were stratified into the same four categories with respect to the observed inversion base as in Section 4.2. The results are presented in Fig. 3. Note that the four categories are not covered by an equal number of cases.

In all four categories of inversion base REMO simulates a vertical temperature stratification at low levels which is more stable than observed. Even in cases of observed elevated inversions surface-based inversions are modelled (categories II and III). In accordance with the overestimated low-level stable stratification in REMO, the relative humidity decreases faster with height than observed (categories III and IV). Wind speeds agree well in the SL, but are too small above the SL in REMO. The same holds for the vertical shear of wind speed and direction.

The differences (REMO minus observation) with respect to vertical stratification and wind shear are striking and systematic (hold for all four categories), but are contradictory from a physical point of view: for the stronger (than observed) low-level stable stratification in REMO one would expect a stronger and not a smaller (than observed) vertical shear of wind speed and direction. To investigate the causes of this contradiction a detailed inspection of the individual terms (including e.g. the divergences of the turbulent and radiation fluxes) in the budget equations of heat and momentum would be necessary both on the model and observational side. On the observational side, however, such an investigation is not possible because radiosondes do not measure turbulent and radiation fluxes.

5.3. Comparison of horizontal ABL structure

The horizontal distribution of the ABL structure was measured during six aircraft missions of RA Falcon during the 1998 winter experiment and during ten aircraft missions of RA DO-128 during the 2001 winter experiment. Each mission represents a snapshot for a 1-2 hours long period. Since each mission was flown during a different weather situation, a comparison between REMO and all aircraft measurements would require a case by case discussion. This would exceed by far the typical size of a paper in this journal. Therefore, we restrict our analysis here to two flight missions of RA

7

DO-128 which represent the two extreme weather situations over the ice-covered Baltic Sea: warm-air advection from southwest and cold-air advection from northeast. These two cases shall demonstrate the horizontal variability of the ABL in nature, and the problems with which REMO – with a horizontal grid resolution of 18 km – is faced. Further examples of the spatial variability of the ABL over sea ice are presented in Brümmer et al. (2002). Observations of two other cases of on-ice and off-ice air flow over the Baltic Sea during the 1998 winter experiment and related simulations with a two-dimensional model are presented in Vihma and Brümmer (2002).

5.3.1. Comparison of a warm-air advection case

The warm-air advection case was observed on 14 February 2001 between 12.10 and 13.10 UTC. The horizontal distribution of surface temperature T_s, sensible heat flux H, and latent heat flux E measured by RA DO-128 at 10 m height and modelled by REMO (data for 13 UTC) are presented in Fig. 4. At 10 m height, the observed wind was FF = 13-18 m s^{-1} from DD = 250-260° and the observed air temperature was T = 3 to 4° C. The surface was covered by 100 % land-fast ice in the north and east and by more than 90 % drift ice in the west and south of the observational area.

Under warm-air advection conditions with air temperatures above 0° C the surface temperatures of open water (sea water freezing temperature T_w = -0.1° C) and melting snow/ice are not very different and, thus, low-level meteorological conditions are rather homogeneous. This situation is well-captured by REMO (Fig. 4) with surface temperatures around 0° C, sensible heat fluxes of H = -20 to -40 W m^{-2} and latent heat fluxes around E = -10 W m^{-2}.

The vertical ABL structure at the southwestern and northeastern edge of the experimental area is compared in Fig. 5. Horizontal homogeneity was also present in the shallow stable ABL above the SL and is represented in REMO. Only the inhomogeneous moisture distribution at levels above the stable ABL is not reproduced in the model. The vertical structure of the shallow stable ABL which is formed when the warm air flows over the cooler surface is not well simulated by REMO. The same deficiencies occur as already detected by comparison with the radiosondes in Figs. 2 and 3: The sharpness of the low-level inversion is not captured in REMO; instead the inversion is smoothed over a several hundred meters thick layer. As a consequence, the shear of wind speed and direction associated with the inversion is also missing in the model simulation.

5.3.2. Comparison of a cold-air advection case

The cold-air advection case was observed on 21 February 2001 between 10.10 and 12.00 UTC. The observed horizontal distributions of T_s, H and E at 10 m height are compared in Fig. 6 with REMO data for 11 UTC. The observed wind was FF = 12-15 m s^{-1} from DD = 60-80° and the observed air temperature was T = -13 to -11° C. Due to the strong northeasterly wind a polynia formed at the edge of the land-fast ice. Drift ice fields were present west of the polynia. The drift ice fields varied in ice concentration and thickness; both were small in the westernmost part of the experimental area.

The inhomogeneous ice conditions are reflected in the T_s observations but not in the REMO simulations, where the ice concentration was prescribed from the gridded FIMR ice maps. As a consequence of the non-real ice conditions the turbulent heat fluxes of H and E disagree, as well. This is a general problem which models face in situations of off-ice cold-air advection if, in nature, ice conditions are inhomogeneous. This problem can only be solved or at least reduced with a better

knowledge of the sea ice conditions (e.g. from satellites) or by coupled atmosphere-ice-ocean models as planned in future runs of the BALTIMOS model.

The vertical ABL structure observed at the northeastern and southwestern edge of the experimental area is compared with the modelled structure in Fig. 7. A strong inversion with h_B around 550 m covered the well-mixed ABL below it. REMO simulates the vertical well-mixed structure and the downwind temperature increase in the ABL well, but fails again in the representation of the sharpness and strength of the topping inversion and the related vertical moisture distribution and wind shear. This deficiency not only appears to be a consequence of the vertical grid resolution (the observed vertical temperature profile can be approximated better than in Fig. 7 even by the use of only 5 grid points below 1000 m in REMO) but also hints at shortcomings in the parameterization of sub-grid processes such as the vertical turbulent fluxes.

6. Summary and conclusions

The regional climate model REMO which is the atmospheric component of the coupled atmosphere-ocean-ice-land system model BALTIMOS is tested with respect to its ability to simulate the SL and ABL structure over the open and ice-covered Baltic Sea realistically. The results of the REMO simulations are compared to in situ observations taken during eight field experiments.

For the comparisons, REMO is run in the so-called forecast mode. REMO forecasts start daily using the 00 UTC ECMWF analyses as initial and boundary conditions. Each forecast covers a period of 30 hours from which the first 6 hours of simulation are neglected. Differences between REMO and observations showed no significant dependence on the forecast time within the 6 to 30 hours integration interval (not shown).

Comparisons of meteorological quantities in the SL over open water show systematically an underestimation/overestimation of downwelling shortwave/longwave radiation flux as a consequence of an overestimatimation of cloud cover in REMO. These findings are supported by the results from comparisons with radiosondes which show that REMO tends to simulate the vertical ABL structure in a certain direction: the ABL inversion is too weak, both in ΔT and Δh. In line with the underestimated vertical stability, too much moisture is found in and above the inversion and the vertical wind shear is underestimated. All these findings hint at a too effective vertical mixing over sea in REMO.

Comparisons in the SL and ABL over land-fast sea ice indicate that, on the average, the SL temperature is too low and the vertical stratification in the lowest 100 or 200 m thick layer is too stable in REMO. The wind shear in this layer is systematically underestimated in spite of the overestimated stability. The reason for this contradiction is unknown and needs further investigation.

REMO simulations of the horizontal variability of the SL and ABL over sea ice were compared with aircraft measurements. Two opposite situations were looked at: warm-air advection from the open water and cold-air advection from the land or ice-covered sea. The observed heterogeneity of the underlying sea ice (concentration, thickness) could not be represented in the REMO simulations. The missing details of ice distribution have no remarkable consequences in case of warm-air advection because ice and water have nearly the same temperature. However, they have large consequences, particularly concerning the heat fluxes in the SL, in case of cold-air advection because the contrasts between ice and water temperature are large.

Taken all comparisons together, the most important finding is that REMO tends to simulate the ABL temperature inversion in a smoothed manner which causes further problems in the vertical moisture distribution and wind shear. The findings in this paper hint at possible deficiencies in the parameterisations of the vertical exchange both under unstable conditions in the ABL over water and sea ice and under stable conditions in the lowest 200 m over sea ice. The representation of inversion sharpness and strength can potentially be improved by increasing the number of vertical grid levels (which is only 6 levels in the lowest 1.2 km). If the inversion simulation will then really be improved depends on the quality of the parameterizations of the subgrid-scale processes (turbulence, clouds, radiation) and on their non-linear interactions.

The problems in the simulation of the ABL over sea ice which emerge from the inhomogeneous sea ice cover can be reduced by a better knowledge of the ice concentration (together with a finer horizontal grid) or by coupling REMO with an ocean/ice model as will be realized in the coupled BALTIMOS model.

References:

BALTEX, 1995: Baltic Sea Experiment BALTEX – Initial Implementation Plan. Internat. BALTEX Secretariat, Publication Series No. 2, pp. 84. ISSN 1681-6471.

Brümmer, B., D. Schröder, J. Launiainen, T. Vihma, A.-S. Smedman, and M. Magnusson, 2002: Temporal and spatial variability of surface fluxes over the ice edge zone in the northern Baltic Sea. J. Geophys. Res., Vol. 107, No. C8, 11/1-16, doi: 10.1029/2001 JC 000884.

Brümmer, B., G. Müller, D. Schröder, A. Kirchgäßner, J. Launiainen, and T. Vihma, 2003: The eight BALTIMOS field experiments 1998-2001 over the Baltic Sea. Internat. BALTEX Secretariat, Publication Series No. 24, pp. 138. ISSN 1681-6471.

Brümmer, B., A. Kirchgäßner, and G. Müller, 2005: The atmospheric boundary layer over Baltic Sea ice. Boundary- Layer Meteorology, No. 117, 91-109.

Jacob, D., 2001: A note to the simulation of the annual and inter-annual variability of the water budget over the Baltic Sea drainage basin. Meteorology and Atmospheric Physics, Vol. 77, Issue 1-4, 61-73.

Jacob, D., U. Andrae, G. Elgered, C. Fortelius, L.P. Graham, S.D. Jackson, U. Karstens, Chr. Koepken, R. Lindau, R. Podzun, B. Rockel, F. Rubel, H.B. Sass, R.N.D. Smith, B.J.J.M. Van den Hurk, X. Yang, 2001: A Comprehensive model intercomparison study investigating the water budget during the BALTEX-PIDCAP period. Meteorology and Atmospheric Physics, Vol. 77, Issue 1-4, 19-43.

Jacob, D. et al., 2006: BALTIMOS – Validation strategy and model performance. Theor. Appl. Climatol., this issue.

Lorenz, P. and D. Jacob, 2006: BALTIMOS – a fully coupled modelling system for the Baltic Sea and its drainage basin. Theor. Appl. Climatol., this issue.

Pirazzini, R., T. Vihma, J. Launiainen and P. Tisler, 2002: Validation of HIRLAM boundary-layer structures over the Baltic Sea. Boreal Env. Res., 7, 211-218, ISSN 1239-6095.

Sorooshian, S., R.G. Lawford, P. Try, W. Rossow, J. Roads, I. Polcher, G. Sommeria, R. Schiffer, 2005: Water and energy cycles: investigating the links, WMO Bulletin, 2005, 1-7.

Tjernström, M., M. Zagar, G. Svensson, J. Cassano, S. Pfeifer, A. Rinke, K. Wyser, K. Dethloff, C. Jones , T. Semmler, M. Shaw, 2005: Modelling the Arctic boundary layer: an evaluation of six ARCMIP regional-scale models using data from the SHEBA project. Boundary- Layer Meteorology, 117 (2), 337-381, doi: 10.1007/s10546-004-7954z.

Uotila, J., T. Vihma and J. Launiainen, 1997: Marine meteorological radiosoundings in the northern Baltic Sea from RV Aranda in 1994-95. Meri-Report Series of the Finnish Institute of Marine Research, Helsinki, No. 30, 57 pages.

Vihma, T. and B. Brümmer, 2002: Observations and modelling of the on-ice and off-ice air flow over the northern Baltic Sea. Boundary- Layer Meteorology, 103, 1-27.

WCRP, 1991: Global Energy and Water Cycle Experiment (GEWEX) Continental Scale International Project: Scientific Plan, WMO/TD-No. 461.

Wyser, K., C.G. Jones, P. Du, E. Girard, U. Willén, J. Cassano, J.H. Christensen, J.A. Curry, K. Dethloff, J.-E. Haugen, D. Jacob, M. Køltzow, R. Laprise, A. Lynch, S. Pfeifer, A. Rinke, M. Serreze, M.J. Shaw, M. Tjernström and M. Zagar, 2007: An evaluation of Arctic cloud and radiation processes during the SHEBA year: simulation results from eight Arctic regional climate models. Clim. Dyn. doi: 10.1007/s00382-007-0286-1.

Figure Captions

Fig. 1: Location of the eight field experiments over the Baltic Sea. The cross marks position of RV Alkor during the six experiments over the open Baltic Sea proper in 2000 and 2001. Rectangles mark area of aircraft operations and letters mark position of surface and radiosonde stations (A = RV Aranda; K, M = coastal stations Kokkola and Marjaniemi) during the two winter experiments 1998 and 2001 over the ice-covered Gulf of Bothnia.

Fig. 2: Average vertical profiles of air temperature T, relative humidity RH, wind speed FF and wind direction DD from REMO (stars) and RV Alkor radiosondes (full line) over the open Baltic Sea for four categories of the observed temperature inversion: surface-based inversion, inversion base < 250 m, inversion base > 250 m and no inversion. Numbers give quantity of profiles used for averaging. Dashed line indicates dry adiabat.

Fig. 3: As Fig. 2, but for the ice-covered Baltic Sea. Comparison is based on radiosondes launched at RV Aranda in 1998 and 2001 and at coastal station Kokkola in 1998.

Fig. 4: Horizontal distribution of surface temperature T_s, sensible heat flux H and latent heat flux E measured at 10 m height by RA DO-128 (12.10-13.10 UTC) and simulated by REMO (13 UTC) for the warm-air advection case on 14 February 2001.

Fig. 5: Vertical profiles of air temperature T, water vapour mixing ratio m, wind speed FF and direction DD measured by RA DO-128 and simulated by REMO at the southwestern (blue) and northeastern edge (red) of the experimental area (see Fig. 4) for the warm-air advection case on 14 February 2001.

Fig. 6: As Fig. 4, but for cold-air advection case on 21 February 2001. Aircraft measurements hold for 10.10-12.00 UTC and REMO simulation for 11 UTC.

Fig. 7: As Fig. 6, but for cold-air advection case on 21 February 2001. Profiles hold for the eastern (blue) and western edge (red) of the experimental area (see Fig. 6).

Quantity		Accuracy	Quantity		Accuracy
Pressure	p	0.2 hPa	Shortwave Radiation	S↓	10 W m^{-2}
Air Temperature	T	0.2 K	Longwave Radiation	L↓	10 W m^{-2}
Sfc Temperature	T_s	0.2 K	Sensitive Heat Flux	H	10 W m^{-2}
Relative Humidity	RH	3-5 %	Latent Heat Flux	E	10 W m^{-2}
Wind Speed	FF	0.3-0.5 ms^{-1}	Momentum Flux	τ	0.05 N m^{-2}
Wind Direction	DD	3-5 °	Cloud Cover	N	1 Octa

Table 1:   Absolute accuracy of meteorological quantities measured at the various platforms.

	Baltic Sea (open water)						
	April 2000	**June 2000**	**Oct. 2000**	**April 2001**	**June 2001**	**Oct. 2001**	**Mean**
No. hourly values	88	85	69	153	135	147	677
Air Pressure p [hPa]	3.2 ± 1.3	2.1 ± 0.9	-1.2 ± 1.3	-0.4 ± 1.6	0.5 ± 1.7	2.8 ± 2.5	1.8
Air Temp. T [K]	0.5 ± 0.5	0.5 ± 0.6	0.8 ± 0.6	-0.4 ± 0.7	-0.1 ± 0.6	-0.6 ± 0.6	0.1
Rel. Humi. RH [%]	-9 ± 7	-4 ± 5	-3 ± 6	4 ± 4	1 ± 4	3 ± 3	0
Sfc. Temp. T_s [°C]	0.7 ± 0.5	0.0 ± 0.4	-0.5 ± 0.5	-0.6 ± 0.3	-1.1 ± 0.7	-0.6 ± 0.4	-0.5
Wind Speed FF [m/s]	0.0 ± 2.0	0.3 ± 2.2	-0.3 ± 2.9	-1.3 ± 1.7	-0.4 ± 1.7	-1.6 ± 3.9	-0.7
Wind Direct. DD [°]	11 ± 14	11 ± 48	7 ± 81	35 ± 48	-13 ± 35	1 ± 13	7
Shortw. Rad. S↓ [W/m²]	-4 ± 103	-76 ± 138	-22 ± 60	-57 ± 110	-42 ± 93	-28 ± 70	-40
Longw. Rad. L↓ [W/m²]	5 ± 32	18 ± 21	15 ± 36	17 ± 27	16 ± 23	8 ± 43	12
Cloud Cover N [%]	/	/	/	67 ± 61	/	44 ± 39	56

Table 2: Mean difference (REMO minus observation) and standard deviation for various quantities measured at RV Alkor during the six field experiments over open water. Last column gives weighted (with number of hours) mean for all experiments.

Experiment	Number of Profiles			Number of Inversions			
	total	with inversions		surface inversions		elevated inversions	
		REMO	Obs.	REMO	Obs.	REMO	Obs.
April 2000	14	3	10	1	3	2	7
June 2000	17	2	7	1	0	1	7
October 2000	16	5	6	0	0	5	6
April 2001	27	27	25	16	19	11	6
June 2001	42	42	40	10	5	32	35
October 2001	38	21	29	3	8	18	21
Sum	154	100	117	31	35	69	82

Experiment	Inv. Base h_B [m]		Inversion Depth Δh [m]				Temperature Difference ΔT [°C]			
	elevated		surface		elevated		surface		elevated	
	REMO	Obs.	REMO	Obs.	REMO	Obs.	REMO	Obs.	REMO	Obs.
April 2000	780	407	103	156	385	76	0.2	1.3	-0.1	0.3
June 2000	318	244	106	-	219	126	0.1	-	-0.6	0.8
October 2000	721	613	-	-	429	133	-	-	-0.2	0.1
April 2001	89	203	283	168	258	94	2.0	3.2	1.5	1.6
June 2001	181	238	431	83	247	130	1.9	1.6	0.8	0.9
October 2001	626	372	715	186	434	74	-1.2	0.1	0.4	0.2
Mean	453	346	328	148	329	106	0.6	1.6	0.3	0.7

Table 3: Comparison of temperature inversion in REMO and observations (Obs.) for the six field experiments over open sea: inversion frequency, inversion base h_B, inversion depth Δh and temperature difference ΔT.

	Baltic Sea (land-fast sea ice)				
	ARA 1998	**KOK 1998**	**ARA 2001**	**MAR 2001**	**Mean**
No. hourly values	438	446	189	262	1335
Air Pressure p [hPa]	-0.8 ± 3.0	-1 ± 2.7	1 ± 1.7	1.5 ± 2.2	-0.2
Air Temp. T [K]	1.1 ± 3.0	-1.5 ± 3.0	-1.1 ± 2.6	-1.0 ± 2.0	-0.5
Rel. Humi. RH [%]	-4 ± 10	5 ± 9	9 ± 9	7 ± 7	3
Sfc. Temp. T_s [°C]	0.4 ± 2.7	-0.1 ± 3.0	0.0 ± 3.0	0.3 ± 2.4	0.3
Wind Speed FF [m/s]	2.0 ± 3.2	0.5 ± 2.3	0.8 ± 1.6	0.8 ± 1.9	1.1
Wind Direct. DD [°]	8 ± 48	-2 ± 43	-13 ± 34	-7 ± 36	-1
Shortw. Rad. S↓ [W/m²]	31 ± 63	-40 ± 72	-17 ± 39	-36 ± 49	-13
Longw. Rad. L↓ [W/m²]	/	-2 ± 36	5 ± 36	-6 ± 28	-2

Table 4: Mean difference (REMO minus observation) and standard deviation for various quantities measured over land-fast sea ice at RV Aranda (ARA), Kokkola (KOK) and Marjaniemi (MAR) during field experiments 1998 and 2001. Last column gives weighted (with number of hours) mean for all stations.
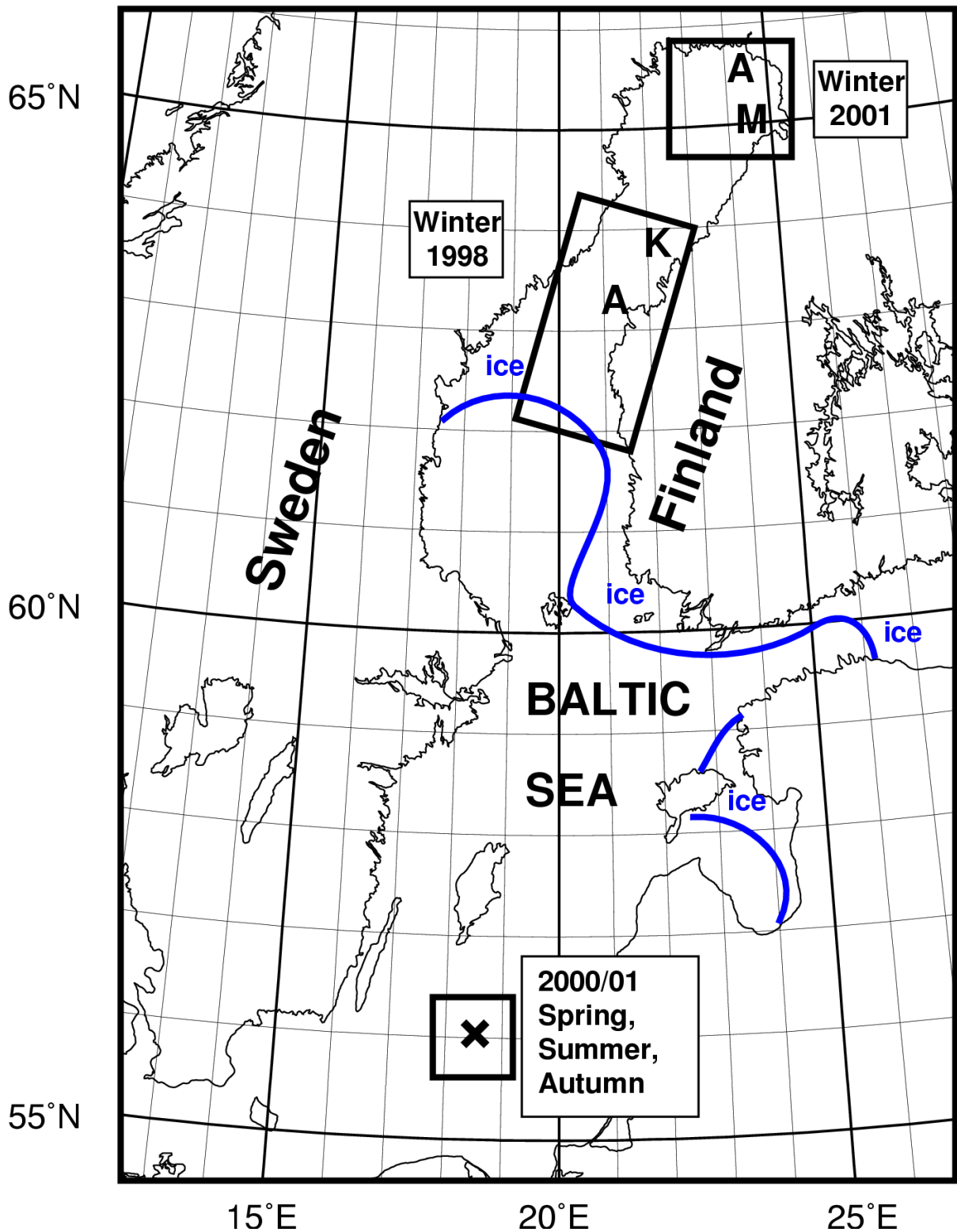
Fig. 1: Location of the eight field experiments over the Baltic Sea. The cross marks position of RV Alkor during the six experiments over the open Baltic Sea proper in 2000 and 2001. Rectangles mark area of aircraft operations and letters mark position of surface and radiosonde stations (A = RV Aranda; K, M = coastal stations Kokkola and Marjaniemi) during the two winter experiments 1998 and 2001 over the ice-covered Gulf of Bothnia.
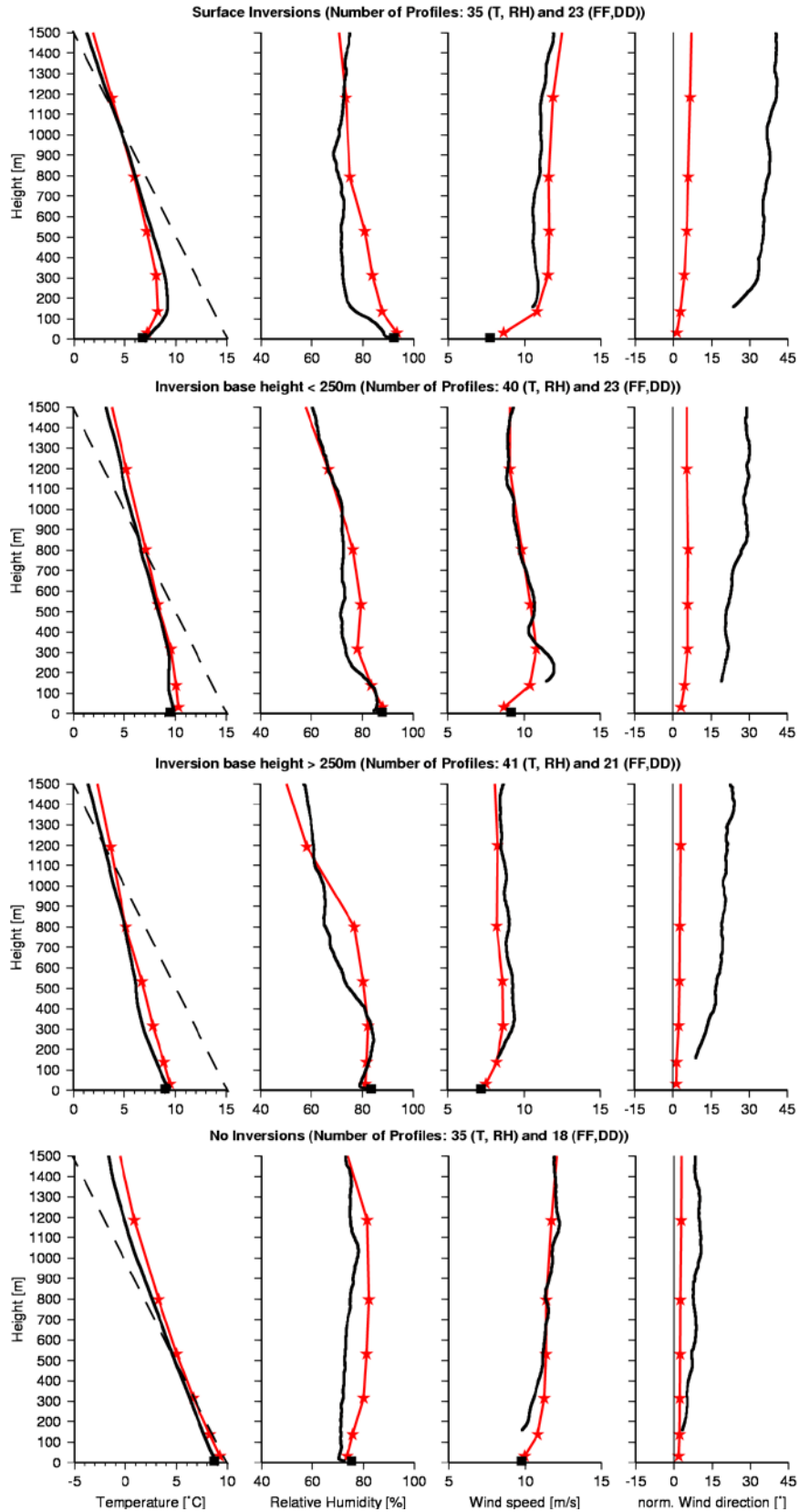
Fig. 2: Average vertical profiles of air temperature T, relative humidity RH, wind speed FF and wind direction DD from REMO (stars) and RV Alkor radiosondes (full line) over the open Baltic Sea for four categories of the observed temperature inversion: surface-based inversion, inversion base < 250 m, inversion base > 250 m and no inversion. Numbers give quantity of profiles used for averaging. Dashed line indicates dry adiabat.
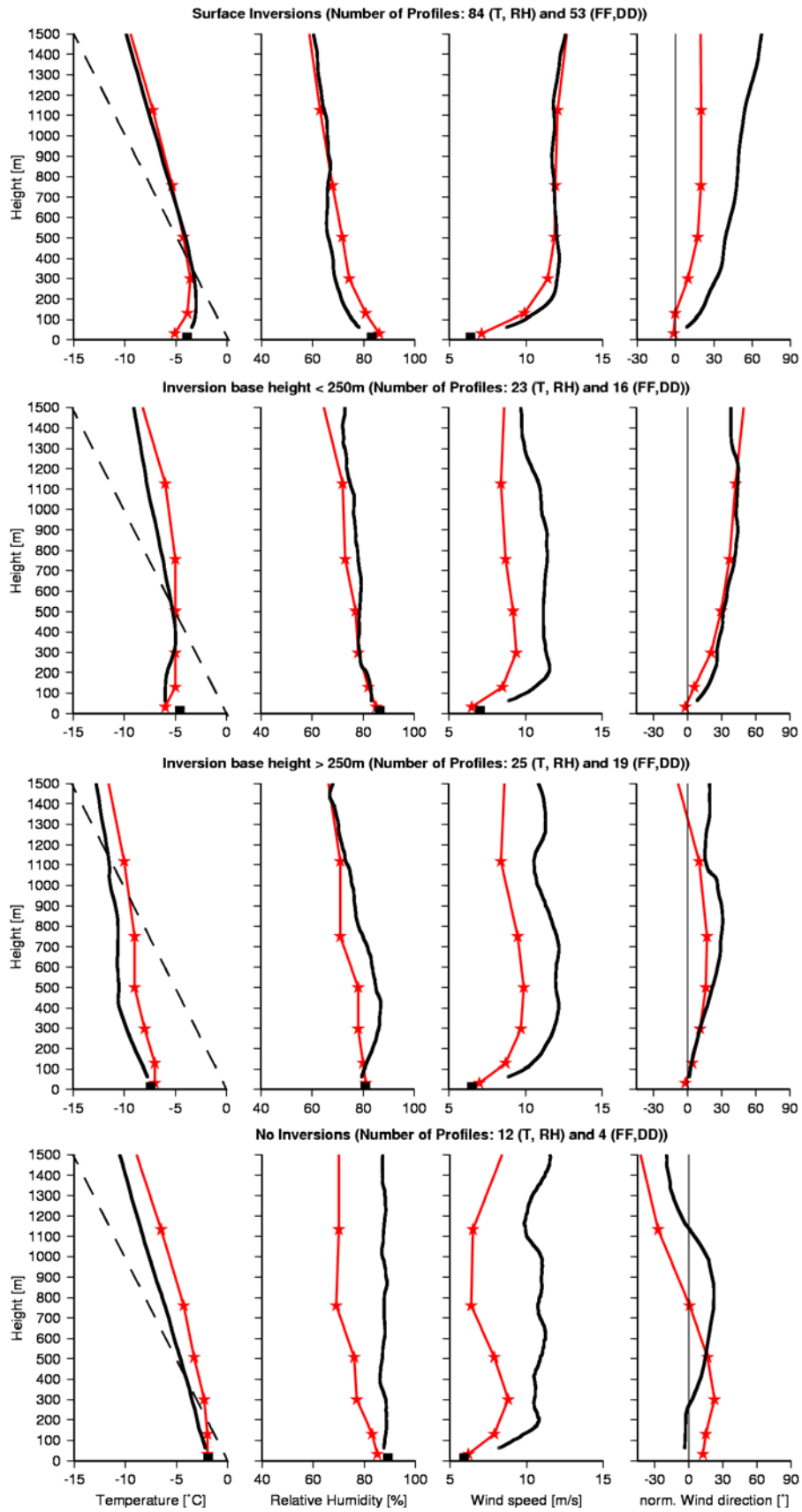
Fig. 3: As Fig. 2, but for the ice-covered Baltic Sea. Comparison is based on radiosondes launched at RV Aranda in 1998 and 2001 and at coastal station Kokkola in 1998.

Fig. 4: Horizontal distribution of surface temperature T_s, sensible heat flux H and latent heat flux E measured at 10 m height by RA DO-128 (12.10-13.10 UTC) and simulated by REMO (13 UTC) for the warm-air advection case on 14 February 2001.
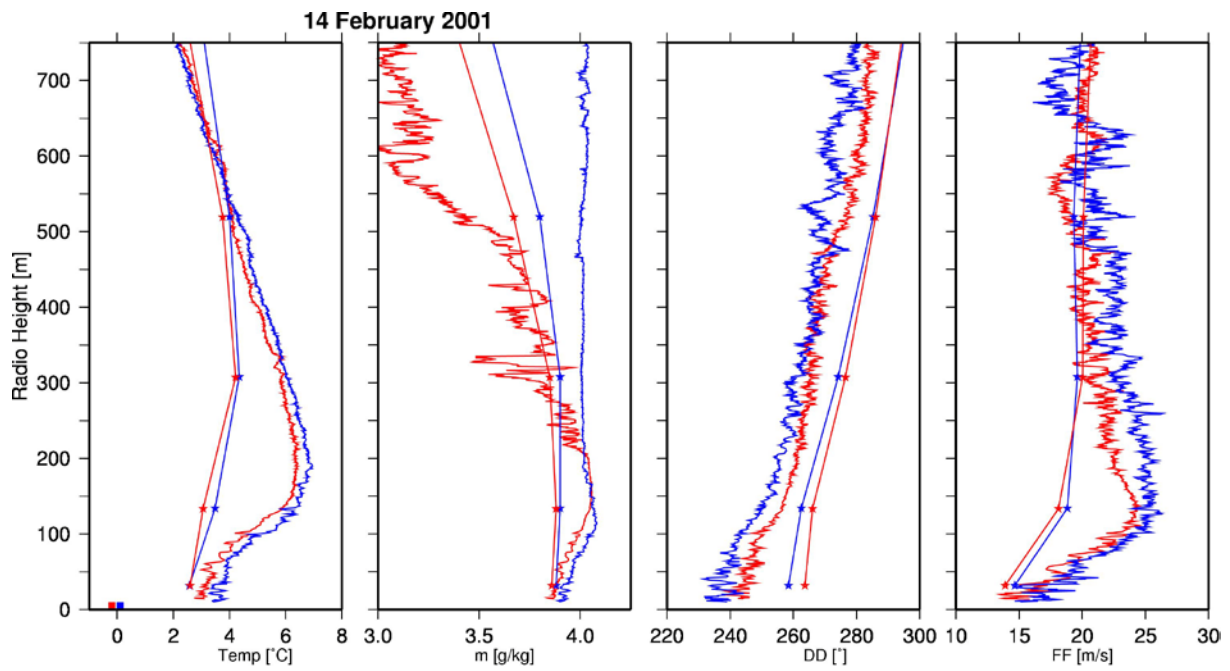
Fig. 5: Vertical profiles of air temperature T, water vapour mixing ratio m, wind speed FF and direction DD measured by RA DO-128 and simulated by REMO at the southwestern (blue) and northeastern edge (red) of the experimental area (see Fig. 4) for the warm-air advection case on 14 February 2001.

Fig. 6: As Fig. 4, but for cold-air advection case on 21 February 2001. Aircraft measurements hold for 10.10-12.00 UTC and REMO simulation for 11 UTC.
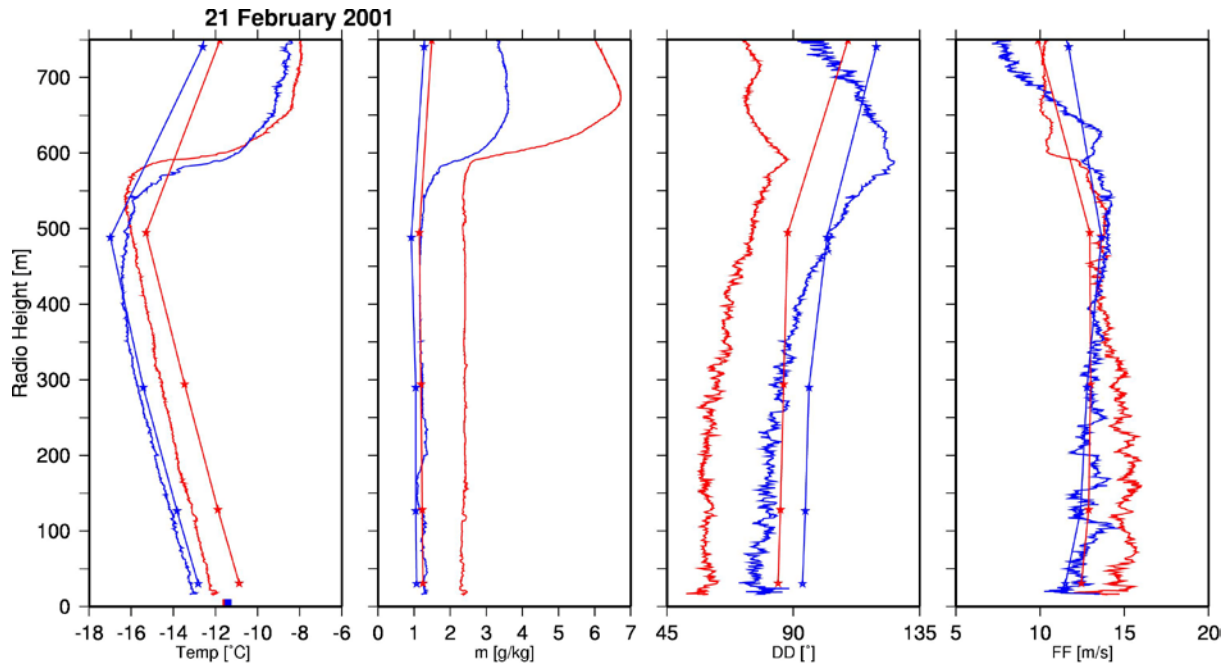
Fig. 7: As Fig. 6, but for cold-air advection case on 21 February 2001. Profiles hold for the eastern (blue) and western edge (red) of the experimental area (see Fig. 6).